



HAL
open science

Thermal cracking of CH₃Cl leads to auto-catalysis of deposited coke

Eugénie Blaser, Cécile Rosier, Michel Huet, Perrine Chaurand, Christophe Geantet, Stéphane Loridant

► **To cite this version:**

Eugénie Blaser, Cécile Rosier, Michel Huet, Perrine Chaurand, Christophe Geantet, et al.. Thermal cracking of CH₃Cl leads to auto-catalysis of deposited coke. *Catalysis Science & Technology*, 2021, 11 (2), pp.469-473. 10.1039/d0cy01725f. hal-03159671

HAL Id: hal-03159671

<https://hal.science/hal-03159671>

Submitted on 28 Sep 2021

HAL is a multi-disciplinary open access archive for the deposit and dissemination of scientific research documents, whether they are published or not. The documents may come from teaching and research institutions in France or abroad, or from public or private research centers.

L'archive ouverte pluridisciplinaire **HAL**, est destinée au dépôt et à la diffusion de documents scientifiques de niveau recherche, publiés ou non, émanant des établissements d'enseignement et de recherche français ou étrangers, des laboratoires publics ou privés.

COMMUNICATION

Thermal cracking of CH₃Cl leads to auto-catalysis of deposited coke

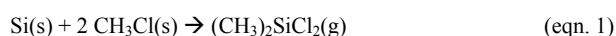
Received 00th January 20xx,
Accepted 00th January 20xx

DOI: 10.1039/x0xx00000x

Eugénie Blaser,^{a,b*} Cécile Rosier,^b Michel Huet,^b Perrine Chaurand,^c
Christophe Geantet,^a and Stéphane Loridant,^{a*}

Thermal cracking of CH₃Cl was studied on SiO₂ particles, at 0.4 MPa, from 375 to 550 °C. The cracking occurs for temperatures higher than 400 °C and leads to the formation of solid coke composed of chlorinated hydrocarbons. This coke is active as it catalyses the CH₃Cl cracking at temperatures lower than those required for the thermal cracking and leads to the formation of HCl, CH₄ and hydrocarbons. Cl present in this coke is responsible for its activation.

In 2019, 2.4 million metric tons of silicones were synthesized¹ and used in a wide range of application (transportation, electronics, energy,...).^{2,3} Therefore, it is crucial to optimize each major step of the silicones production such as the direct synthesis, also called the Müller-Rochow reaction and given in eqn. 1.



In this reaction, solid silicon is mixed with gaseous CH₃Cl at temperature and pressure ranging between 265-310 °C and 2-7 bar, respectively, in fluidized-bed reactors.^{4,5} Copper-based catalysts are usually used to increase the selectivity to (CH₃)₂SiCl₂ and give a long steady state.^{6,7,8} However, the Direct Synthesis suffers from a side-reaction during which the CH₃Cl reagent cracks and forms H₂, HCl, CH₄ as well as solid and liquid hydrocarbons.^{9,10} These hydrocarbons, usually referred to as coke, may deposit on the active sites,¹¹ reduce the productivity of (CH₃)₂SiCl₂ leading to the deactivation.¹² A X-ray micro computed-tomography (micro-CT) image of coke covering the metals-based phases which catalyzed the Direct Synthesis is shown in Figure 1.

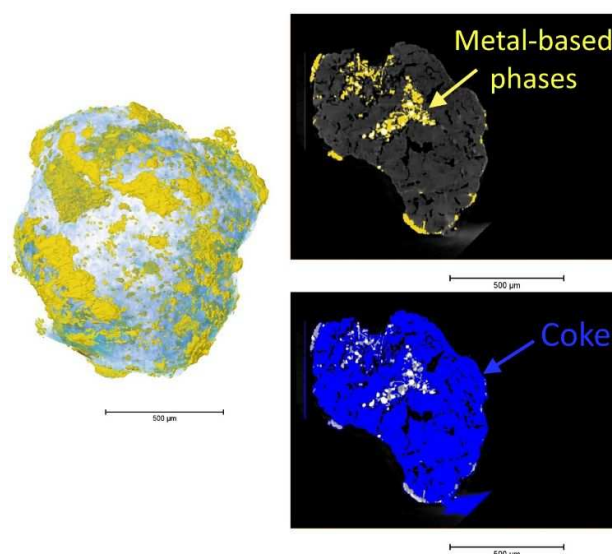


Fig. 1: Virtual 2D slice (right) extracted from the 3D image (left) obtained by micro-CT (1µx=1.95 µm) of solid masses recovered from the Direct Synthesis. Distribution of coke and metal-based phases was obtained by gray threshold segmentation.

High temperatures may cause the thermal cracking of CH₃Cl. This type of cracking was studied by several authors who reported a radical mechanism of CH₃Cl cracking leading to CH₃• and Cl• radicals.¹³⁻¹⁶ However, they used experimental conditions different from those of the Direct Synthesis with temperature much higher than 265-310 °C. Therefore, their conclusions on thermal cracking may not be applied to what occurs in the Direct Synthesis.

In the present work, thermal cracking of CH₃Cl was studied with experimental conditions as close as possible to those of the Direct Synthesis, between 375 and 550 °C. To our best knowledge, no study of thermal cracking in this range of temperature has been reported yet. For each cracking test

^a Univ Lyon, Université Claude Bernard-Lyon 1, CNRS, IRCELYON-UMR 5256, 2av. A. Einstein, F-69626 Villeurbanne Cedex, France, email : stephane.loridant@ircelyon.univ-lyon1.fr and eugenie.blaser@elkem.com

^b ELKEM SILICONES – 55 av Frères Perret 69190 SAINT FONS – France

^c Aix Marseille Univ, CNRS, IRD, INRA, Coll France, CEREGE, Aix-en-Provence, France

(experimental conditions detailed in the ESI), the selectivity values to H_2 , CH_4 , coke and other hydrocarbons with $C \leq 4$ were determined. The purposes of this work were to determine the onset temperature for the CH_3Cl cracking and the reaction of cracking with experimental conditions close to those applied for the Direct Synthesis. Besides, the coke formed by thermal cracking was characterized by C and H elemental analysis, Raman spectroscopy and XRF (methods in the ESI) and tested to determine its catalytic role on the cracking reaction itself.

The tests of CH_3Cl cracking were performed in a fixed-bed reactor (see details in the ESI) with glass beads and silica particles as surface to initiate radicals as well as on black carbon (see materials in the ESI).

The first series of thermal cracking tests was performed on the glass beads and Figure 2 plots the evolution of the CH_3Cl conversion with time. The cracking starts between 400 and 450 °C suggesting it does not occur for the Direct Synthesis performed around 300 °C. Nevertheless, in industrial reactors, insufficient fluidisation may lead to the formation of hot spots¹⁷ where thermal cracking could still occur. This highlights that, with optimal conditions of fluidization, no thermal cracking occurs whereas with inefficient fluidization, coke may be formed by thermal cracking leading to the deactivation and to a production loss.

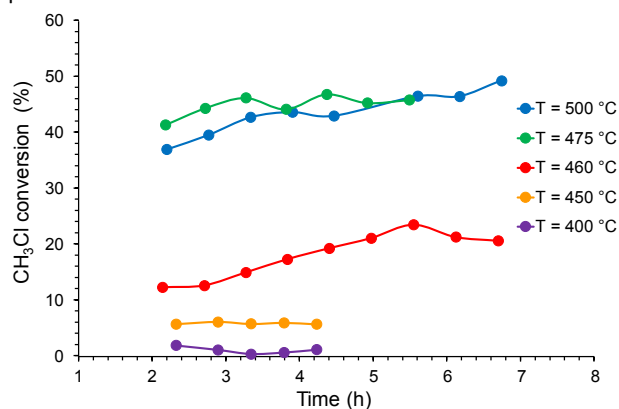


Fig. 2: Conversion of CH_3Cl for thermal cracking on 0.8 g of glass beads ($2m^2/kg$) at 0.4 Mbar. Residence time = 0.3 min. The relative experimental error of the $X(CH_3Cl)$ conversion was estimated at $\pm 0.11 \times X(CH_3Cl)$.

Above 475 °C, the CH_3Cl conversion did not increase with the temperature. This limitation is attributed to the small surface of glass beads. Thus, SiO_2 particles with a higher specific surface area ($310 m^2/g$) were used to study the thermal cracking as well.

The activation energy was determined from the rates of CH_3Cl consumption at different temperatures (Table 1 with rates in the range of 10^{-7} mol/s). The evolution of $\ln(r)$ as function of $1/T$ is reported in Figure 3, with r the consumption rate of CH_3Cl . Only the temperatures 450, 460 and 475 °C were used for the graph. The rate obtained at 400 °C was too low to be precisely measured and limitation occurred at 500 °C due to the low specific area. From results reported in Table 1, the activation energy was determined at 338 kJ/mol. This result is in the range

of activation energy experimentally determined for the thermal cracking: 305 and 501 kJ/mol.¹⁸ Moreover, the result is close to the dissociation energy of the C-H bond and is lower than the one of C-Cl in CH_3Cl , 339 and 423 kJ/mol respectively.¹⁹ Such result is consistent with a homolytic bond breaking, leading to the radicals formation. However, it does not necessarily mean that only the C-H bond breaks and not C-Cl. CH_3Cl cracking by C-Cl bond breaking was also reported.¹³⁻¹⁵

Table 1: Rate of CH_3Cl consumption for the thermal cracking on glass beads, determined between 2 and 4 h.

Temperature (°C)	Rate of CH_3Cl consumption (mol_{CH_3Cl}/s) $\times 10^7$
400	< 0.1
450	0.4
460	0.8
475	2.5
500	3.0

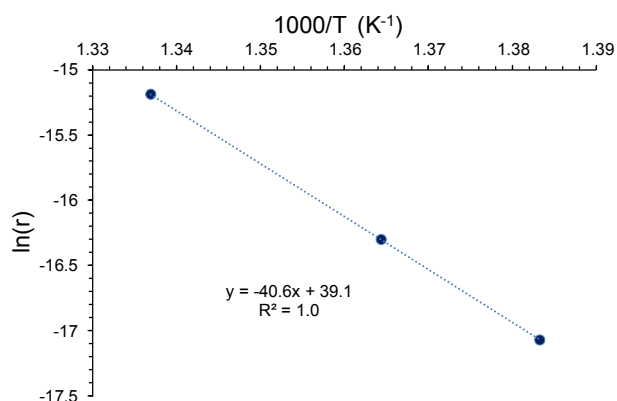


Fig. 3: Arrhenius plot of the thermal cracking of CH_3Cl on glass beads.

The second series of CH_3Cl cracking was performed on silica particles and Figure 4 displays the evolution of CH_3Cl conversion for these tests. Like the glass beads, the cracking starts between 400 and 450 °C.

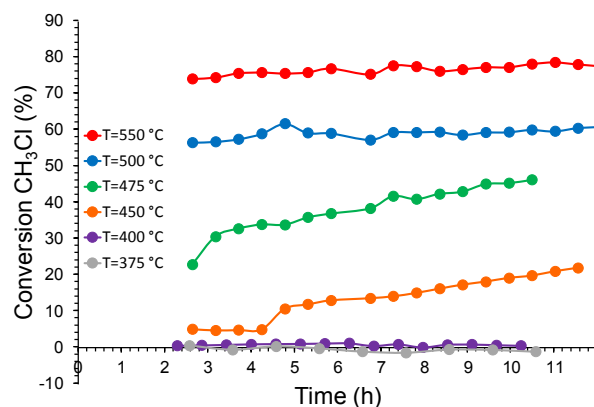


Fig. 4: CH_3Cl conversion for thermal cracking on SiO_2 particles from 375 to 550 °C with 0.8 g of mass loaded, at 0.4 Mbar. Residence time = 0.3 min. The experimental error of the $X(CH_3Cl)$ conversion was estimated at $\pm 0.11 \times X(CH_3Cl)$.

The cokes obtained from thermal cracking at 450, 500, 550 °C and from the Direct Synthesis have a H/C molar ratio of 1.0, 0.2, 0.1 and 0.5, respectively. This suggests the formation of hydrogen-poor coke, which was confirmed by Raman

spectroscopy, displayed in Figure 5. The G-band around 1575–1580 cm^{-1} corresponds to a vibrational mode of graphitic plan with E_{2g} symmetry.^{20,21} The D-band, around 1350 cm^{-1} is due to a vibrational mode with A_{1g} symmetry and is related to defects or heteroatoms present in the graphitic plans.²¹ The ratio $\frac{\text{Area (D - band)}}{\text{Area (G - band)}}$ is related to the order degree of graphite.²¹ This ratio is 2.8 and 3.0 for coke from thermal cracking coke and Direct Synthesis, respectively. The nature of coke obtained by thermal cracking is like the one formed during the Direct Synthesis.

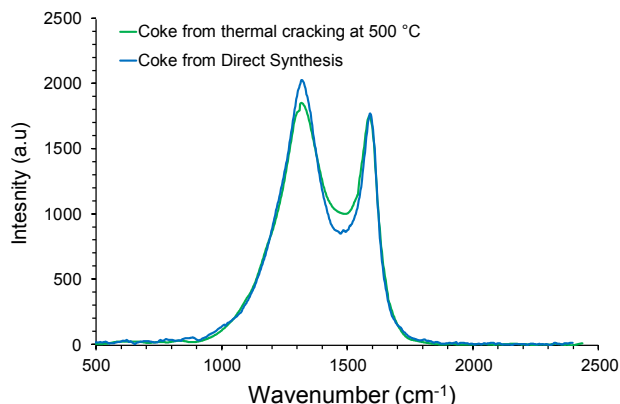


Fig.5: Raman spectra of coke from thermal cracking ($T=500\text{ °C}$) and from Direct Synthesis.

According to Figure 4, the conversion of CH_3Cl tends to increase with time, suggesting the formation of another contributor to the cracking. To estimate the influence of this other cracking contributor, the rate of CH_3Cl consumption and the activation energy between 2 and 4 h and between 8 and 10 h under flow were compared. However, the reaction rate determined at 550 $^{\circ}\text{C}$ was not considered for the calculation of the activation energy because it slowly increases with time suggesting a diffusion resistance. Figure 6 plots the evolution of $\ln(r)$ as function of $1/T$, with r the CH_3Cl consumption rate and the activation energy values are reported in Table 2. The activation energy decreases during the reaction and is much lower than the one obtained with glass beads (i.e. 338 kJ/mol). Such observation suggests the formation of a catalyst during the cracking.

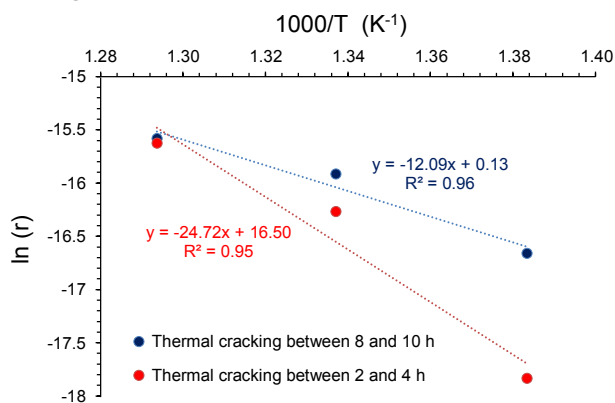


Fig.6: Arrhenius plot corresponding to the beginning and the end of the thermal cracking of CH_3Cl on SiO_2 particles.

Table 2: Rate of CH_3Cl consumption for the thermal cracking on 0.8 g of SiO_2 particles, $P = 0.4$ Mbar, residence time = 0.3 min.

	Rate of CH_3Cl consumption ($\text{mol}_{\text{CH}_3\text{Cl}}/\text{s}$) $\times 10^7$		
	2-4 h	8-10 h	
Temperature ($^{\circ}\text{C}$)	450	0.2	0.7
	475	0.9	1.5
	500	1.6	2.0
	550	2.4	2.5
Activation energy (kJ/mol)	205	100	

To confirm the hypothesis of an auto-catalytic cracking, a reaction was performed on SiO_2 particles at 500 $^{\circ}\text{C}$ and the temperature was decreased to 400 $^{\circ}\text{C}$ after 15 h. Figure 7 compares the CH_3Cl conversion during this test and the one on SiO_2 at 400 $^{\circ}\text{C}$ on fresh silica. While CH_3Cl did not crack on fresh silica at 400 $^{\circ}\text{C}$, it did on SiO_2 after thermal cracking at 500 $^{\circ}\text{C}$, confirming the formation of active compounds for CH_3Cl cracking. Similar results were obtained when the thermal cracking was first performed at 450 and 550 $^{\circ}\text{C}$ instead of 500 $^{\circ}\text{C}$. These results are provided in Figure S1 (see ESI).

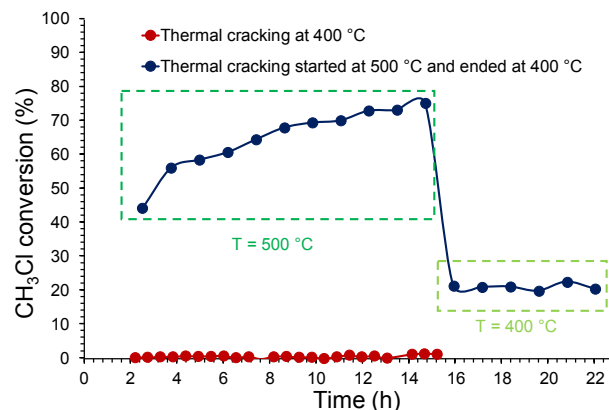


Fig.7: Conversion of CH_3Cl for thermal cracking on 0.8 g of SiO_2 started at 500 $^{\circ}\text{C}$ and ended at 400 $^{\circ}\text{C}$, at 0.4 Mbar and with a residence time of 0.3 min.

To determine whether silica texture contributes or not to this phenomenon, the same test of cracking was performed on larger quartz particles (1 mm). After 15 h of thermal cracking at 500 $^{\circ}\text{C}$, the temperature was reduced at 400 $^{\circ}\text{C}$ and CH_3Cl did crack. This suggests that SiO_2 was not the catalyst for the CH_3Cl cracking since the geometric surface of quartz was too small to generate active sites. Therefore, it appears that coke formed by the thermal cracking further catalyzes the cracking at 400 $^{\circ}\text{C}$. Hence, there is an auto-catalytic phenomenon occurring during the thermal cracking caused by coke and two origins of the cracking have to be distinguished: thermal and auto-catalytic,

with a respective contribution dependent on the temperature. For the industrial Direct Synthesis, it means that coke catalyses the CH_3Cl cracking at temperature lower than those required for the thermal cracking.

Tran et al. reported an auto-catalytic effect for pyrolysis of CH_3Cl on quartz particles but with experimental conditions far from those of the Direct Synthesis (i.e. between 747 and 987 °C, at 1 atm).¹⁸ However, they did not investigate the nature of the catalyst. To our best knowledge, such catalytic activity at 400 °C of coke formed during the CH_3Cl cracking was not previously reported.

The CH_3Cl cracking was performed on black carbon at 400 °C and no cracking was observed. To understand the difference in the activity of black carbon and coke at 400 °C, both solids were compared by Raman spectroscopy (Figure 8). Based on these results, no significant difference was observed between the two solids. In addition, the molar ratio H/C of coke from thermal cracking and black carbon are 0.2 and 0.1, respectively. These results did not explain the difference in activity of both solids.

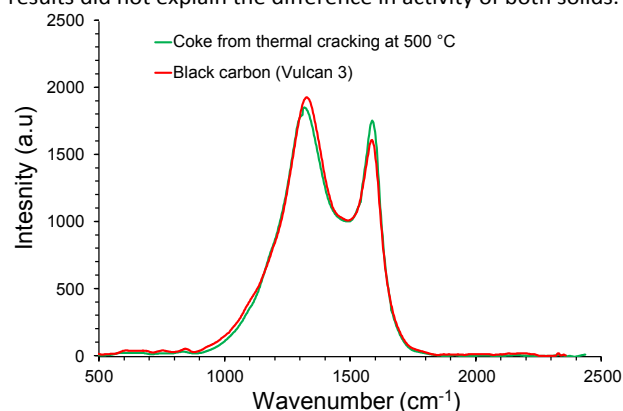


Fig. 8: Raman spectra of black carbon and thermal coke obtained by CH_3Cl thermal cracking on SiO_2 particles at 500 °C.

XRF performed on cokes obtained at 450, 500 and 550 °C showed the presence of Cl between 1.0 and 7.6 wt%, while the initial Cl content from the SiO_2 support is 0.1 wt%. Cl may acidify the coke, and thus, lead to the formation of acidic sites. Chlorination of activated carbon by Cl_2 ²² or by HCl ²³ is reported to decrease its PZC (Potential of Zero Charge). This means that the acidity of activated carbon increases which is consistent with the hypothesis suggested above. Besides, the higher the temperature for the chlorination, the higher the Cl content in the final solid.^{22,24}

The CH_3Cl consumption rate determined at 400 °C of the cokes obtained by thermal cracking at 450, 500 and 550 °C is related to their initial Cl content, as shown in Figure 9. This confirms the active role of Cl in the auto-catalytic cracking.

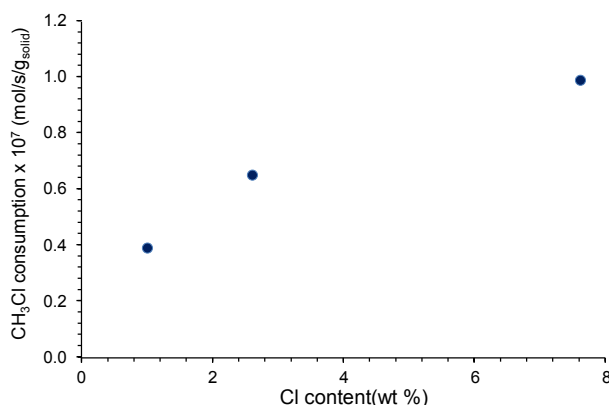


Fig. 9: CH_3Cl consumption rate at 400 °C on thermal coke as function of the Cl content in these cokes obtained by thermal cracking at 450, 500 and 550 °C.

To determine the auto-catalytic reaction of CH_3Cl , focus was put on the selectivity. Thermal cracking at 550 °C was performed to produce a high amount of thermal coke which generates auto-catalytic cracking. The values of selectivity obtained for the whole reaction were as follows: $S(\text{H}_2)$, $S(\text{C}_2)$, $S(\text{C}_3)$, $S(\text{C}_4) < 1\%$, $S(\text{CH}_4) = 44\%$, $S(\text{coke}) = 56\%$, $S(\text{HCl}) \approx 100\%$. Therefore, the reaction eqn. 2 is suggested for the auto-catalytic cracking of CH_3Cl on coke.



Interestingly, this reaction is reported to be the reaction of thermal cracking at temperatures lower than 150 °C, based on thermodynamic simulations.¹⁰ However, since the thermal cracking starts between 400 and 450 °C, it is limited by kinetic below 150 °C but is catalyzed by chlorinated coke at 400 °C.

Conclusions

The thermal cracking of CH_3Cl on inert particles starts between 400 and 450 °C. Therefore, thermal cracking may occur during the industrial Direct Synthesis in hot spots, usually formed with inefficient fluidization. It leads to the formation of an active coke which further catalyses the cracking at 400 °C leading to formation of additional coke (autocatalytic phenomenon). This work also evidenced that coke contains Cl which is at the origin of its catalytic activity.

Conflicts of interest

There are no conflicts to declare.

Acknowledgment

Dr. Cécile Rosier and Michel Huet are acknowledged for initiating this project. Eugénie Blaser thanks Elkem for Ph.D. grant.

Notes and references

- 1 <https://www.imarcgroup.com/silicones-market>
- 2 C. Corden, B. Tyrer, H. Menadue, J. Calero, J. Dade and R. Leferink, Socio-economic evaluation of the global silicones industry, 2013, 4–7.
- 3 W. Kalchauer and B. Pachaly, Handbook of Heterogeneous Catalysis, 2008, 2635–2647.
- 4 B. Kanner and K. Lewis, Catalyzed direct reactions of silicon, Elsevier, 1993.
- 5 J. Mohsseni, J. Gross, K. Mautner, N. Sofina and T. Wuestenfeld, US Patent 0305939, Method for the Direct Synthesis of Methylchlorosilanes in Fluidized-bed reactors 2017.
- 6 C. Wang, G. Wang and J. Wang, *Chin. J. Chem. Eng.*, 2014, **22**, 13, 299–304.
- 7 A.D. Gordon, B.J. Hinch and D.R. Strongin, *J. Catal.*, 2009, **266**, 291–298.
- 8 Y. Zang, J. Li, H. Lui, Z. Zhong and F. Sun, *Chem. Cat. Chem.*, 2019, **12**, 2757–2779.
- 9 V. Bazant, *Pure Appl. Chem.*, 1966, **13**, 1313, 313–326.

- 11 C. Bartholomew, *Appl. Catal. A*, 2001, **212**, 17–60.
- 12 J. Jokilk and V. Bazant, *Collect. Czech Chem. C*, 1961, **26**, 417–426.
- 13 A. Shilov and R. Sabirova, *Russ. J. Phys. Chem. A*, 1959, **34**, 408–411.
- 14 O. Kondo, K. Saito and I. Murakami, *Chem. Soc. Jpn.*, 1980, **53**, 2133–2140.
- 15 M. Weissman and S. W. Benson, *Int. J. Chem. Kinet.*, 1984, **16**, 307–333.
- 16 Y.-S. Won, *J. Ind. Eng. Chem.*, 2007, **3**, 400–405.
- 17 Z. Jia, C. Zhang, D. Cai, E. Blair, W. Qian and F. Wei, *RSC Adv.*, 2017, **7**, 20186–20191.
- 18 T. Tran and S. Senkan, *Ind. Eng. Chem. Res.*, 1994, **33**, 32–40.
- 19 J. A. Dean, Lange's Handbook of Chemistry, McGraw-Hill, Inc, 1999, 308–310.
- 20 A. Cuesta, P. Dhamelinourt and J. Laureyns, *Carbon*, 1994, **32**, 18, 1523–1532.
- 21 M. Pimenta, G. Dresselhaus, M. Dresselhaus, L. Cançao, A. Jorio and R. Saito, *Phys. Chem. Chem. Phys.*, 2007, **9**, 1276–1291.
- 22 A.-F. Perze-Cadenas, F. Maldonado-Hodar and M. Moreno-Castill, *Carbon*, 2003, **41**, 473–478.
- 23 M. Evans, E. Halliop, S. Liang and J. MacDonald, *Carbon*, 1988, **36**, 111, 1677–1682.
- 24 R. Hall and R. Holmes, *Carbon*, 1993, **31**, 16, 881–886.

Electronic Supplementary Information for

Thermal cracking of CH₃Cl leads to auto-catalysis of deposited coke

Eugénie Blaser, Cécile Rosier, Michel Huet, Perrine Chaurand , Christophe Geantet and Stéphane Loridant

Univ Lyon, Université Claude Bernard Lyon 1, CNRS, IRCELYON, F-69626, Villeurbanne, France

Materials

As the thermal cracking of CH₃Cl was reported to be a radical route, two types of inert surface were used to initiate the CH₃• and Cl• radicals. The first one consisted of glass beads purchased from Carl Roth (Ref. A555.1) with a size ranging between 1.25 and 1.65 mm and with a geometric area of 2 m²/kg. The second inert surface was SiO₂-432 from Grace Davison, crushed and sieved between 50 and 400 μm before the CH₃Cl cracking. Its specific surface area (SSA) was 310 m²/g and it contained 0.1 wt% of Cl. Black Carbon was a Vulcan 3 (Cabot) powder sample with SSA of 75 m²/g.

Catalytic testing for the thermal cracking

The CH₃Cl cracking tests were performed in a fixed-bed reactor with a height and a diameter of 3 and 1 cm, respectively. All the tests were performed at a pressure of 0.4 MPa (similar to the DS) and six temperatures were set: 375, 400, 450, 475, 500 and 550 °C.

Before each test, the reactor was flushed under 100 mls/min of pure Ar at atmospheric pressure while temperature was increased from room temperature to the desired one with a rate of 5 °C/min and maintained under Ar for 1 h. The argon flush was then stopped. CH₃Cl/Ar (10/90) mixed with N₂, with respective flow of 5.22 and 3.18 mls/min, were introduced during ca 15 h. N₂ was used as an internal standard.

During the CH₃Cl cracking, the output gases N₂, CH₃Cl, H₂, CH₄, C₂H₆, C₂H₄, C₃H₈, C₃H₆, n-butane and isobutene were analyzed by Shimadzu GC-2014 and treated with the LabSolutions software. HCl selectivity was determined using a trap with NaOH and by measuring the initial and final pH.

The selectivity to A product was calculated by (eqn. S1).

$$\text{Sel (A)} = \frac{n(\text{A})_{\text{output}}}{n(\text{CH}_3\text{Cl})_{\text{input}} - n(\text{CH}_3\text{Cl})_{\text{output}}} \times 100 \quad (\text{eqn. S1})$$

where $n(\text{A})_{\text{output}}$ corresponds to the amount of A product at the output of the fixed bed reactor and $n(\text{CH}_3\text{Cl})_{\text{input}}$ and $n(\text{CH}_3\text{Cl})_{\text{output}}$ correspond to the amount of CH₃Cl reagent on the input and output of the fixed bed reactor, respectively.

The consumption rate of CH₃Cl was calculated by (eqn. S2) with $X(\text{CH}_3\text{Cl})$ the conversion of CH₃Cl and $F(\text{CH}_3\text{Cl})$ the input flow of CH₃Cl (mol.s⁻¹). A first-order of reaction was assumed for the calculation of the reaction rate, because of the low partial pressure of CH₃Cl.

$$r_{\text{CH}_3\text{Cl consumption}} = X(\text{CH}_3\text{Cl}) \times F(\text{CH}_3\text{Cl}) \quad (\text{eqn. S2})$$

The activation energy of thermal cracking was determined from the rates determined after two hours of reaction assuming a first order reaction. For glass beads, the experiments performed at 400 ° and 500 °C were discarded because the conversion was too low and limitation occurred, respectively. For silica particles, the experiment performed at 550 °C was not considered for the calculation because diffusion resistance was suspected.

Characterization methods

In addition to gases, the amount of coke deposited on silica was determined by elemental analysis on carbon with a Thermo Scientific, Flash 200 organic elemental analyzer.

Raman spectra reported in this work were performed at ambient atmosphere with a LabRam HR (Jobin Yvon-Horiba) spectrometer. The exciting line at 633 nm of a He-Ne laser was used. The power measured at the sample was around 1 mW. The spatial resolution is ca 4 microns and the spectral resolution is 4 cm⁻¹. For each sample, the spectrum corresponds to the mean of ca 20 spectra recorded on different analysis areas.

The X-Ray Fluorescence analysis was performed with a Panalytical, Epsilon 4 instrument equipped with an Ag source. The Cl content was determined from a semi-quantitative method (Omnian).

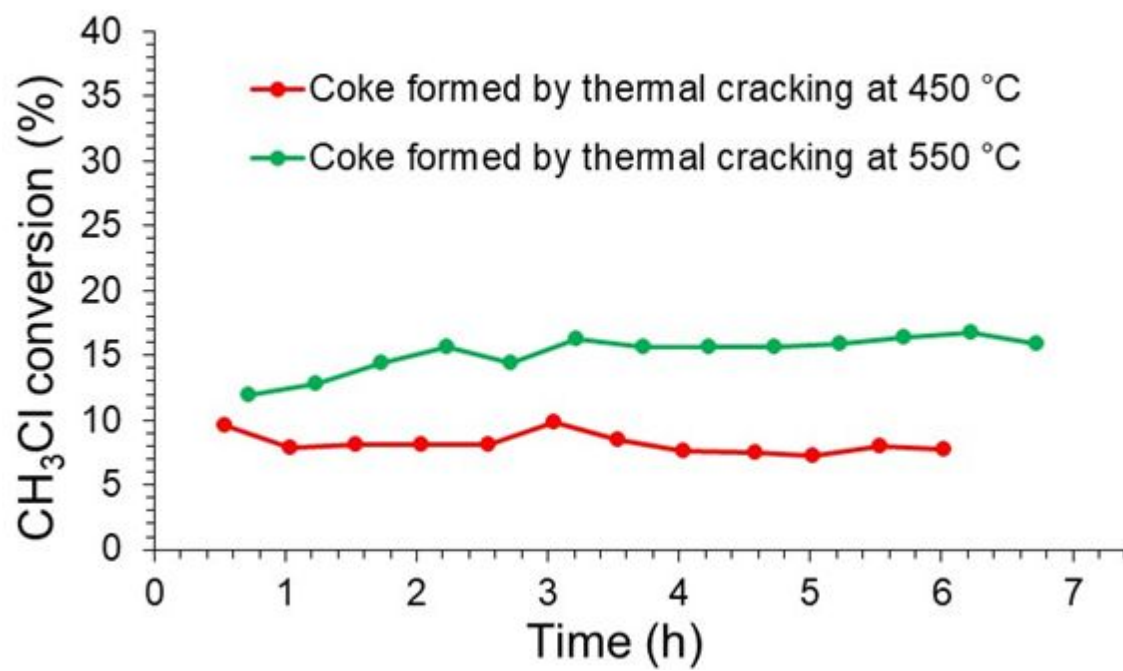


Fig. S1: Conversion of CH₃Cl at 400 °C on coke obtained by thermal cracking on 0.8 g of SiO₂ at 450 and 550 °C, at 0.4 Mbar and with a residence time of 0.3 min.

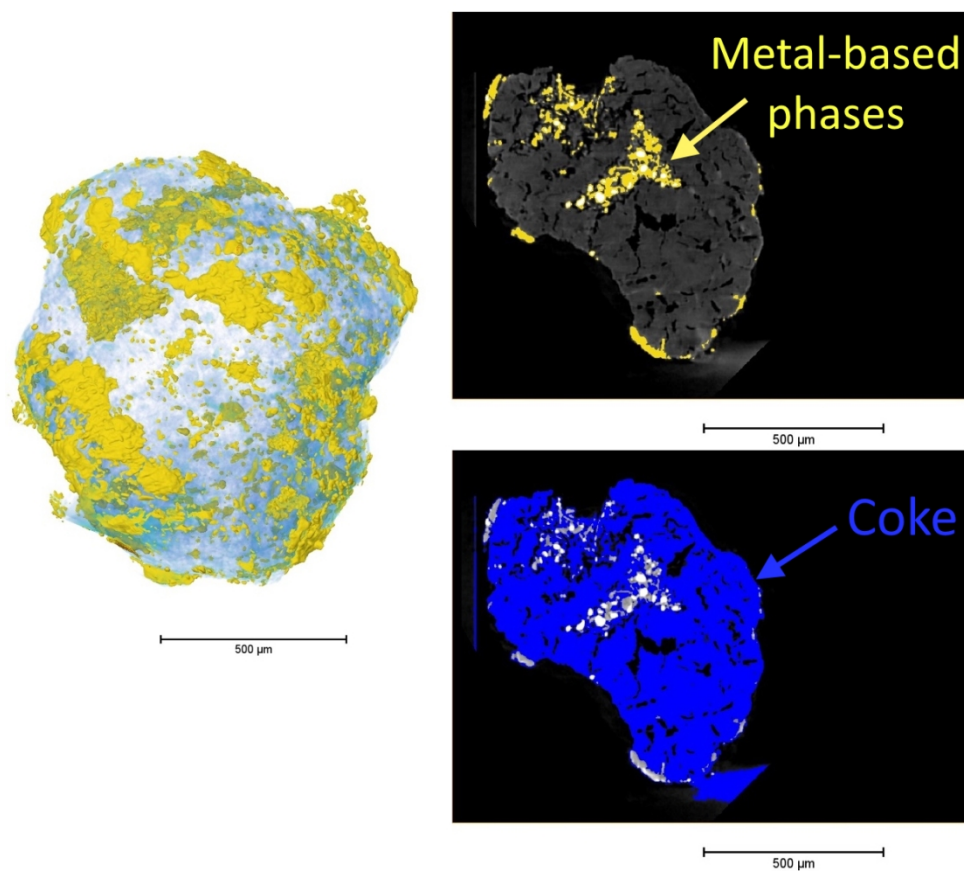


Figure 1

150x138mm (220 x 220 DPI)

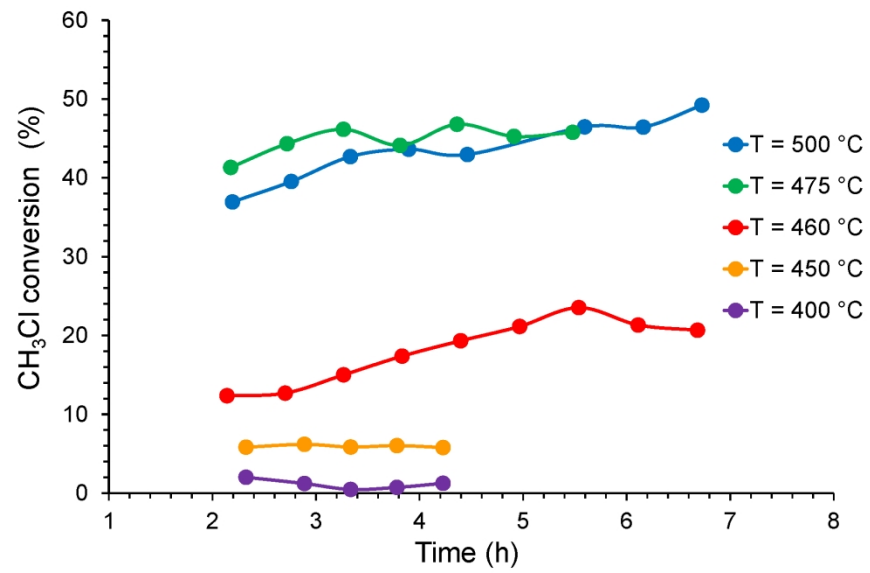


Figure 2

297x210mm (200 x 200 DPI)

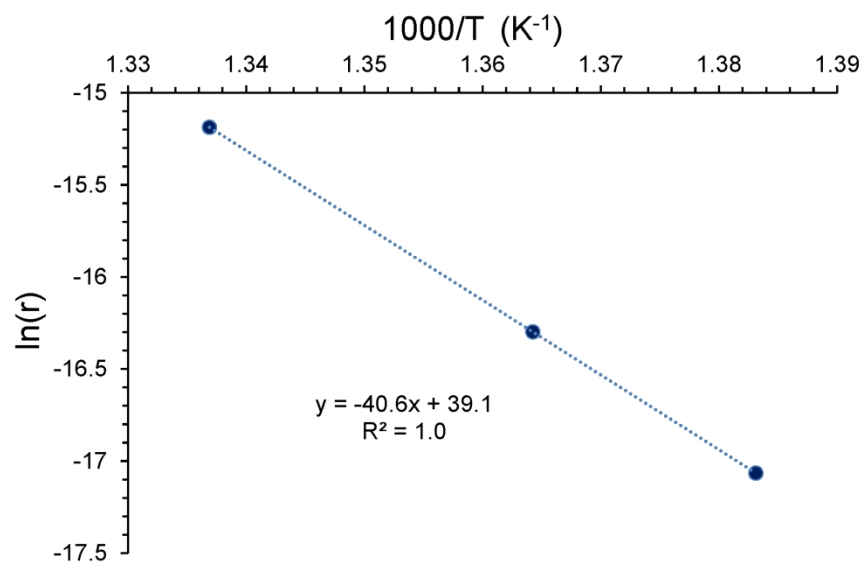


Figure 3

297x210mm (200 x 200 DPI)

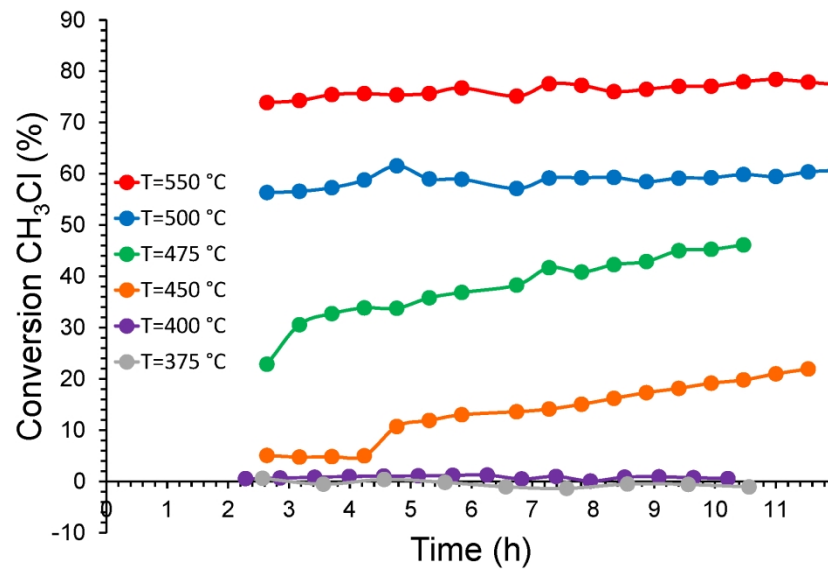


Figure 4

297x210mm (200 x 200 DPI)

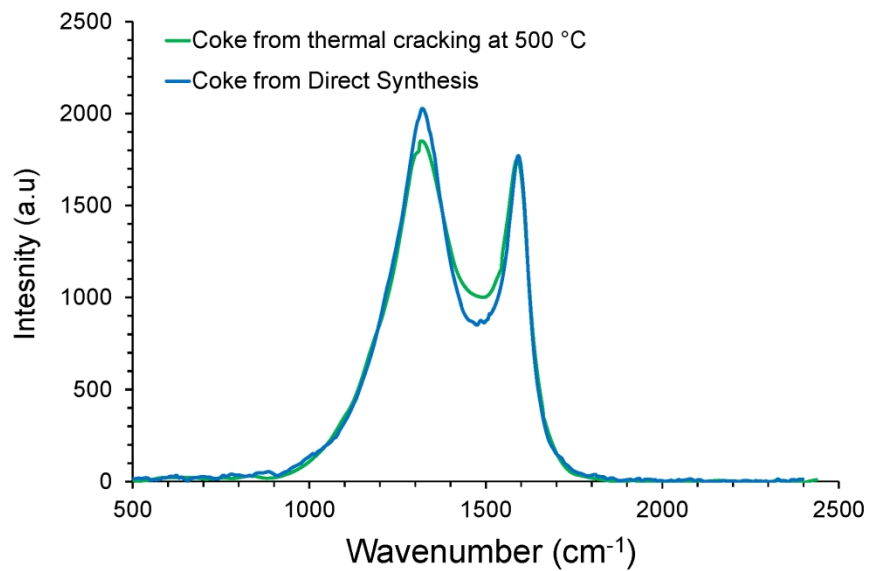


Figure 5

297x210mm (200 x 200 DPI)

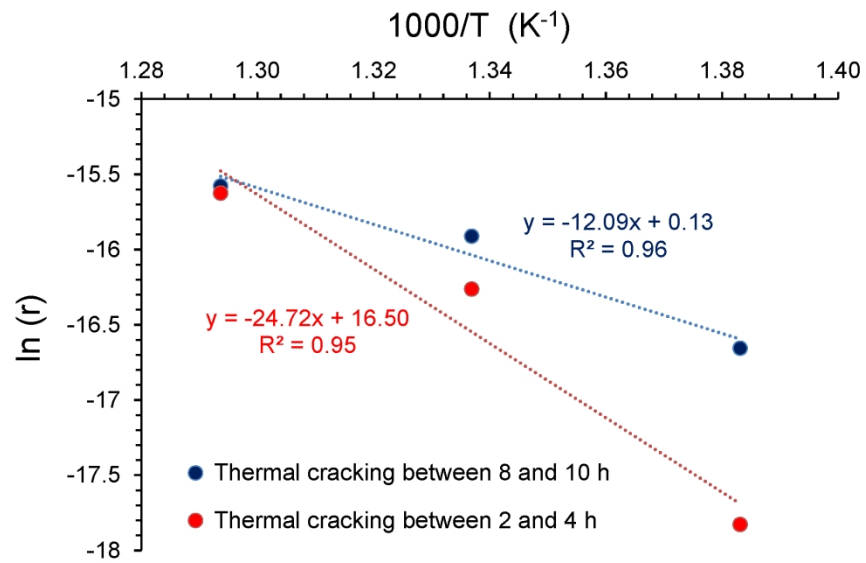


Figure 6

297x210mm (200 x 200 DPI)

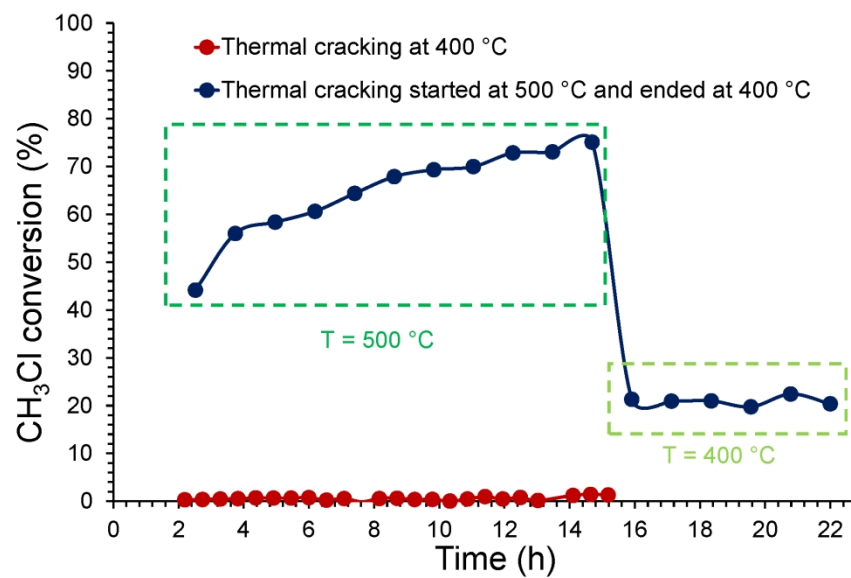


Figure 7

297x210mm (200 x 200 DPI)

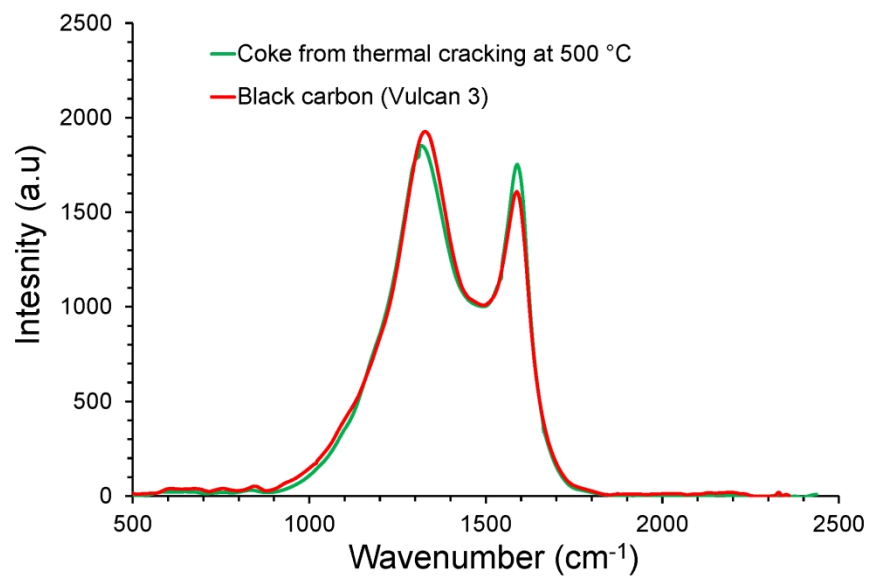


Figure 8

297x210mm (200 x 200 DPI)

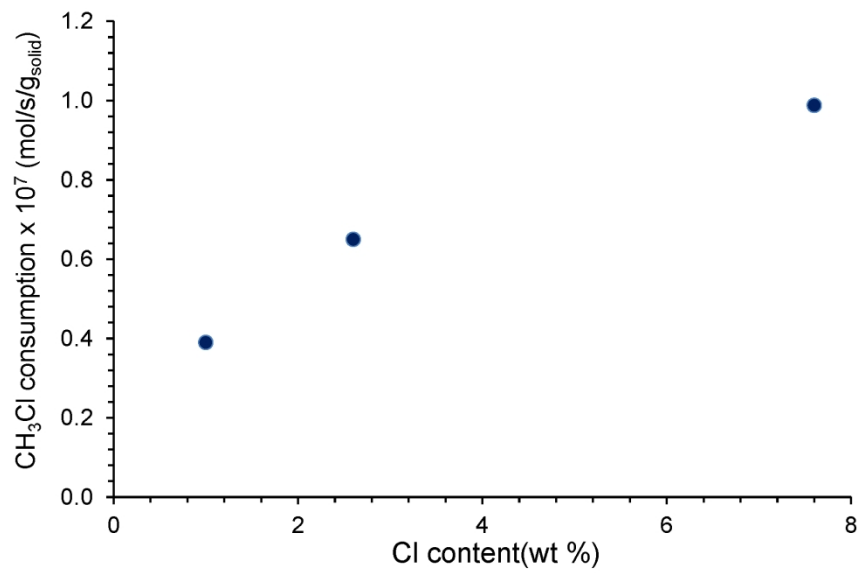
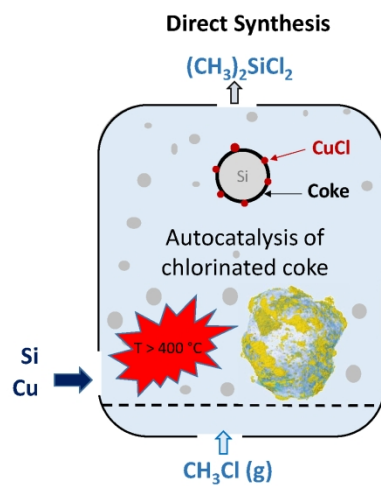


Figure 9

297x210mm (200 x 200 DPI)



297x210mm (220 x 220 DPI)